# Lithosphere

*Research Article*

# A New Multi-Objective Comprehensive Optimization Model for Homogeneous Slope Reinforced by Anti-Slide Piles: Insights from Numerical Simulation

**Chao Xu,**[1,2,3] **Lei Xue** (ID) **,**[1,2,3] **Yuan Cui,**[1,2,3] **Songfeng Guo,**[1,2,3] **Mengyang Zhai,**[1,2,3] **and Fengchang Bu**[1,2,3]

[1]*Key Laboratory of Shale Gas and Geoengineering, Institute of Geology and Geophysics, Chinese Academy of Sciences, Beijing 100029, China*
[2]*Innovation Academy for Earth Science, Chinese Academy of Sciences, Beijing 100029, China*
[3]*College of Earth and Planetary Sciences, University of Chinese Academy of Sciences, Beijing 100049, China*

Correspondence should be addressed to Lei Xue; xuelei@mail.iggcas.ac.cn

Landslides have posed a huge threat to the ecological environment and human society all over the world. As the most conventional reinforcement method, anti-slide piles are widely used in the reinforcement of slopes. Currently, more and more attention has been paid to the low-cost and high-efficiency optimal design of anti-slide piles. However, limitations in the method of the optimization design for slopes reinforced with piles still exist. In this paper, a new multi-objective comprehensive optimization method was proposed for the optimization of the slope reinforced with anti-slide piles. The factor of safety, internal force, and deflection of piles were selected as the optimization indexes, and the optimization index weight was determined by integrating the subjective and objective weights. The influence of pile locations, pile lengths, and pile spacings on the reinforcement effect of a homogeneous slope was analyzed via the numerical simulation. Through the simulation case analysis, the proposed model had achieved good effects on the optimization design of anti-slide piles, which could effectively reduce the engineering costs. The optimization results showed that the best reinforcement effect for the homogeneous slope could be obtained when the anti-slide piles with the critical pile length and small pile spacing were located in the middle of the slope. This provides a new solution for the optimization design of other types of complex slopes and has broad application prospects.

## 1. Introduction

With the rapid development of global engineering construction, slope stability has become a worldwide significant problem in engineering practice [1, 2]. The anti-slide piles as the most conventional reinforcement method are widely used due to the advantages of strong anti-sliding ability and convenient construction [3–5]. Therefore, the design of anti-slide piles is crucial. At present, the mainstream design methods for anti-slide piles include the loading-structure method [6], Viggiani method [7], Ito Tomio method [8], and Poulos method [9], which are based on limit equilibrium or displacement compatibility. The basic

idea for these methods is to determine the residual pushing force and anti-slide force satisfied with the stability of the slope firstly, then calculate the bending moment and shear force for each pile, and finally give the suitable design parameters such as the pile length, the pile spacing, and the pile location [5]. However, these methods fail to consider the interaction between pile and soil, which cannot accurately reflect the true stability of the slope-pile system.

Recently, more and more scholars [3, 10–12] have realized the fact that the pile length, pile location, pile spacing, and other design parameters have a significant impact on the reinforcement of the slope via limit equilibrium methods and finite element methods. For example, the optimization
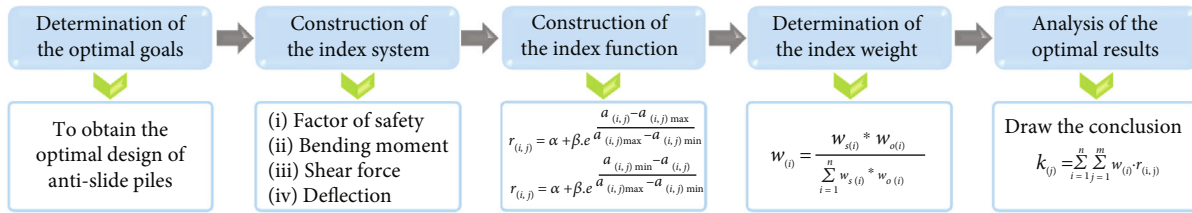
FIGURE 1: Flowchart of the multi-objective comprehensive optimization model.

results of pile length show that there is a critical pile length that can achieve the optimal reinforcement effect, and excessive pile length cannot increase the factor of safety of the slope but will cause construction waste [11, 13–15]. The researches on pile location reveal the fact that the best slope reinforcement effect can be obtained when the anti-slide pile is located in the middle of the slope [2, 3, 12, 16, 17]. Wei and Cheng [4] even gave the precise pile location which is 0.2 m above the middle of the slope. The studies about optimal pile spacing show that the smaller spacing of the anti-slide pile is, the better integrity of the reinforced slope is, which is more conducive to the stability of the reinforced slope [3, 18, 19], but the determination of pile spacing mainly depends on the soil arching effect between piles in practical engineering. Although these studies have a guiding significance for the optimization design of anti-slide piles, the optimization results may have some certain deviations which are because only the factor of safety of reinforced slope is taken as the only optimization objective.

In fact, the slope reinforced with piles is a complete organism composed of the slope and anti-slide piles. Numerous cases of reinforced slope instability [20, 21] show that the optimization design for anti-slide piles needs to consider not only the stability of the slope but also the safety of anti-slide piles. Therefore, it is particularly important to consider the internal force and deformation of the pile in the optimization design process. Yang et al. [22] and Wang et al. [23] revealed the internal force and deformation characteristics of piles under various reinforcement schemes and pointed out that the pile may not be in a safe state when the slope obtained the maximum factor of safety. Zhu et al. [24] fully considered the change of pile head displacement and established the deformation prediction model for anti-slide piles, which provided theoretical guidance for optimal design. However, their studies failed to consider the coordination and contradiction of various pile elements and give qualitative optimization results. Moreover, the analytic hierarchy process (AHP) [25] and multi-objective comprehensive evaluation method [26] were used to optimize the design of anti-slide piles based on the evaluation indexes considered the factor of safety and internal force of piles comprehensively, which is concordant with practical situation.

In conclusion, it is unreasonable to ignore the safety state of anti-slide piles to evaluate the stability of the slope reinforced. Therefore, in this paper, the multi-objective comprehensive optimization model based on improved fuzzy comprehensive evaluation was developed to optimize the design of anti-slide piles, and the optimization indexes sys-

tem and the comprehensive index weight were established, the factor of safety, bending moment, shear force, and deflection were selected as the optimization indexes. FLAC$^{3D}$ software was used to establish a three-dimensional numerical model which could reflect the interaction between the slope and piles to analyze the changes in factor of safety and the internal force and deformation of anti-slide piles under various reinforcement schemes, and the proposed method was used to optimize. Thus, the proposed optimization model is expected to provide a reference for the optimization design of anti-slide pile engineering.

## 2. Multi-Objective Comprehensive Optimization Model

*2.1. Feasibility of the Method.* Generally, most engineering optimization design problems are multi-objective optimization problems, and there are usually contradictions between various optimization objectives. Therefore, the results of optimization design based on a single factor merely are unreliable. The multi-objective comprehensive optimization model takes the research object as a whole, which has the following advantages: (1) it can comprehensively consider the mutual influence between various factors and (2) it can quantify the impact of indexes on optimization goals. In fact, the optimization design of anti-slide piles to strengthen the slope is a multi-objective optimization problem, which could be solved reliably by the multi-objective comprehensive optimization model.

*2.2. Optimization Design Process and Method.* Figure 1 shows the flowchart of the multi-objective comprehensive optimization model based on an improved fuzzy comprehensive evaluation method.

*2.2.1. Determination of the Optimal Goals.* In the design of slope reinforced with anti-slide piles, factors such as pile location, pile length, and pile spacing are usually considered to achieve a good reinforcement effect. However, the overly conservative design has led to high engineering costs in most cases [27]. Therefore, the optimum design of anti-slide piles aims to reduce as many engineering costs as possible while satisfying the safety of supporting structures without affecting the stability of the reinforced slope.

*2.2.2. Construction of the Optimization Index System.* The stability of slopes, the safety of supporting structures, and the economy must be taken into account in the selection of evaluating index system, which will determine the accuracy
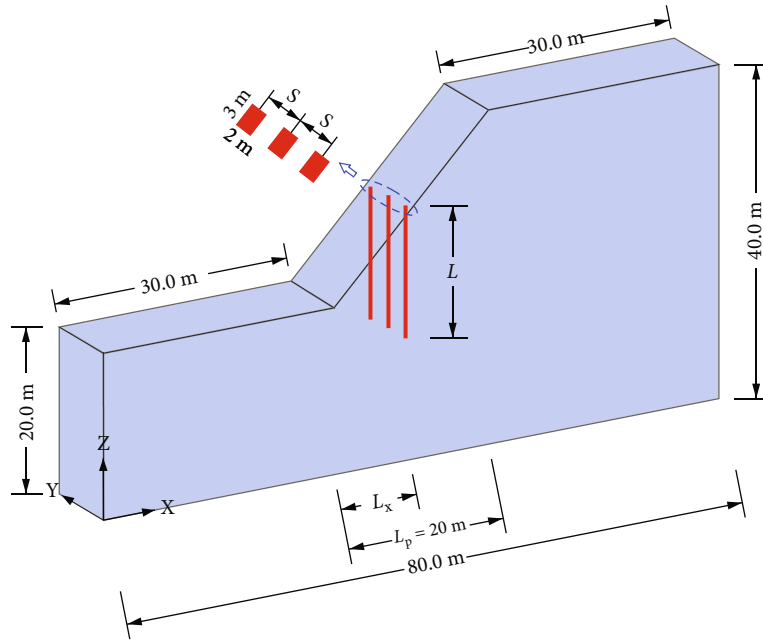
FIGURE 2: Numerical model of slope reinforced with anti-slide piles. $L_x$, $L_p$, $L$, and $S$ stand for the distance from the pile to the slope toe, the horizontal length of the slope, the pile length, and the pile spacing, respectively. For interpretation of the references to color in this figure, the reader is referred to the electronic version of this page.

TABLE 1: Physical and mechanical parameters of the slope.

| Material | Young modulus $E$ (MPa) | Poisson ratio $\nu$ | Unit weight $\gamma$ (kN/m$^3$) | Cohesion $c$ (kPa) | Friction angle $\varphi$ (°) |
|---|---|---|---|---|---|
| Soil | 200 | 0.25 | 20 | 24 | 24 |

of the optimization model. The index of safety factor reflects the stability of a slope reinforced with piles; the indexes of bending moment, internal force, and deflection reflect the safety of anti-slide piles. The changes of the above indicators correspond to different optimization schemes (such as different pile locations, pile lengths, and pile spacings) and will have an obvious impact on the construction difficulty and engineering cost. Therefore, the factor of safety, bending moment, shear force, and deflection of anti-slide piles are selected as the main optimization indexes in this paper.

*2.2.3. Construction of the Index Function.* Suppose that there are $n$ optimization indexes to compose a sample set of optimization indexes $\{a_{(i,j)}|i = 1 \sim n, j = 1 \sim m\}$ for all $m$ schemes. In order to make the data highly comparable and the modeling universal, this study adopts the percentage system [28] and the maximum-minimum standardization method to standardize the evaluating indexes $a_{(i,j)}$.

The standardized formula for the positive optimization indexes that are positively correlated with the results, such as the factor of safety, can be taken as follows:

$$r_{(i,j)} = \alpha + \beta \cdot e^{\left(a_{(i,j)} - a_{(i,j)\,\max}\right)/\left(a_{(i,j)\,\max} - a_{(i,j)\,\min}\right)}, \quad (1)$$

The standardized formula for the negative optimization indexes that are negatively correlated with the results, such as
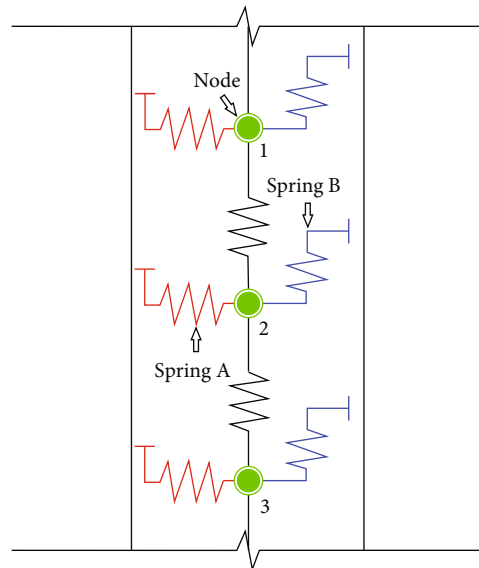


FIGURE 3: Mechanical model of pile (modified after Wang et al. [23]). Spring A and spring B stand for the normal coupling spring and the shear coupling spring, respectively. For interpretation of the references to color in this figure, the reader is referred to the electronic version of this page.

TABLE 2: Physical and mechanical parameters of anti-slide piles.

| Parameter | Value | Parameter | Value | Parameter | Value |
|---|---|---|---|---|---|
| Young modulus (GPa) | 30 | Coupling-cohesion-shear (MPa) | 19 | Coupling-cohesion-normal (MPa) | 19 |
| Poisson ratio | 0.21 | Coupling-stiffness-shear (MN/m$^2$) | 100 | Coupling-stiffness-normal (MN/m$^2$) | 100 |
| Moi-$z$ (m$^4$) | 2.0 | Coupling-friction-shear (°) | 22 | Coupling-friction-normal (°) | 22 |
| Moi-$y$ (m$^4$) | 4.5 | Density (kg/m$^3$) | 2500 | Coupling-gap-normal | On |
| Moi-polar (m$^4$) | 6.5 | Cross-sectional-area (m$^2$) | 6.0 | Perimeter (m) | 10 |

as internal force and deflection of piles, can be taken as follows:

$$r_{(i,j)} = \alpha + \beta \cdot e^{\left(a_{(i,j)\ min} - a_{(i,j)}\right) / \left(a_{(i,j)\ max} - a_{(i,j)\ min}\right)}, \qquad (2)$$

where $a_{(i,j)\ min}$ and $a_{(i,j)\ max}$ are the minimum and maximum values of the $i$th index in the $j$th scheme, respectively; $r_{(i,j)}$ is the standardized optimization value, that is, the relative membership value of the $i$th index in the $j$th scheme is subordinate to the optimal value; and $\alpha$ and $\beta$ are constant indicators for constructing the percentile system which meets $\alpha + \beta = 100$.

Thus, the fuzzy matrix can be determined as follows:

$$R = \begin{bmatrix} r_{(1,1)} & r_{(1,2)} & \cdots & r_{(1,m)} \\ r_{(2,1)} & r_{(2,2)} & \cdots & r_{(2,m)} \\ \vdots & \vdots & & \vdots \\ r_{(n,1)} & r_{(n,2)} & \cdots & r_{(n,m)} \end{bmatrix}_{n \times m}, \qquad (3)$$

*2.2.4. Determination of Index Weight.* The subjective weight determined by the AHP and objective weight determined by the entropy method are used to establish the comprehensive weight of optimization indexes. Thus, the comprehensive weight of evaluating index can be obtained as follows:

$$w_{(i)} = \frac{w_{s(i)} \cdot w_{o(i)}}{\sum_{i=1}^{n} w_{s(i)} \cdot w_{o(i)}}, \qquad (4)$$

where $w_{s(i)}$ and $w_{o(i)}$ are the subjective weight and objective weight, respectively. The objective weight $w_{o(i)}$ can be calculated as follows:

$$w_{o(i)} = \frac{1 - e_{(i)}}{\sum_{i=1}^{n} \left(1 - e_{(i)}\right)}, \qquad (5)$$

where $e_{(i)}$ is the entropy of the $i$th optimization index.

*2.2.5. Analysis and Comparison of the Optimization Results.* The fuzzy comprehensive optimization value $k_{(j)}$ can be obtained by synthesizing the weight of each optimization
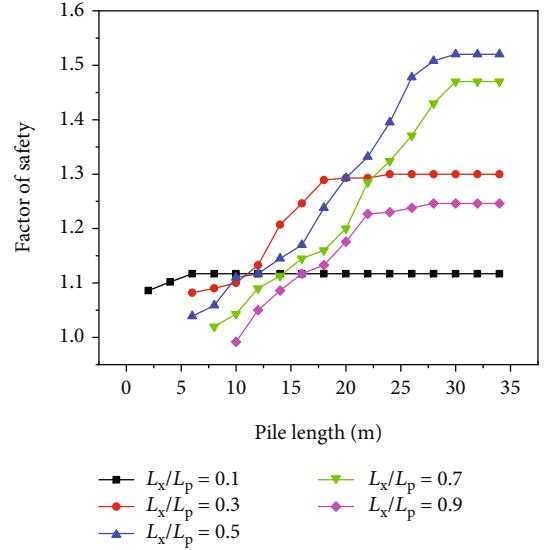


FIGURE 4: Factors of safety for various pile lengths and pile locations. For interpretation of the references to color in this figure, the reader is referred to the electronic version of this page.
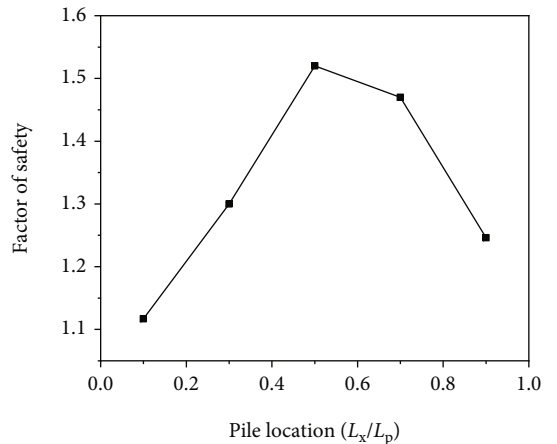


FIGURE 5: Maximum factor of safety for various pile locations.

index $w_{(i)}$ and the relative membership value $r_{(i,j)}$ of the corresponding optimization index in different schemes.

$$k_{(j)} = \sum_{i=1}^{n} \sum_{j=1}^{m} w_{(i)} \cdot r_{(i,j)}, \qquad (6)$$
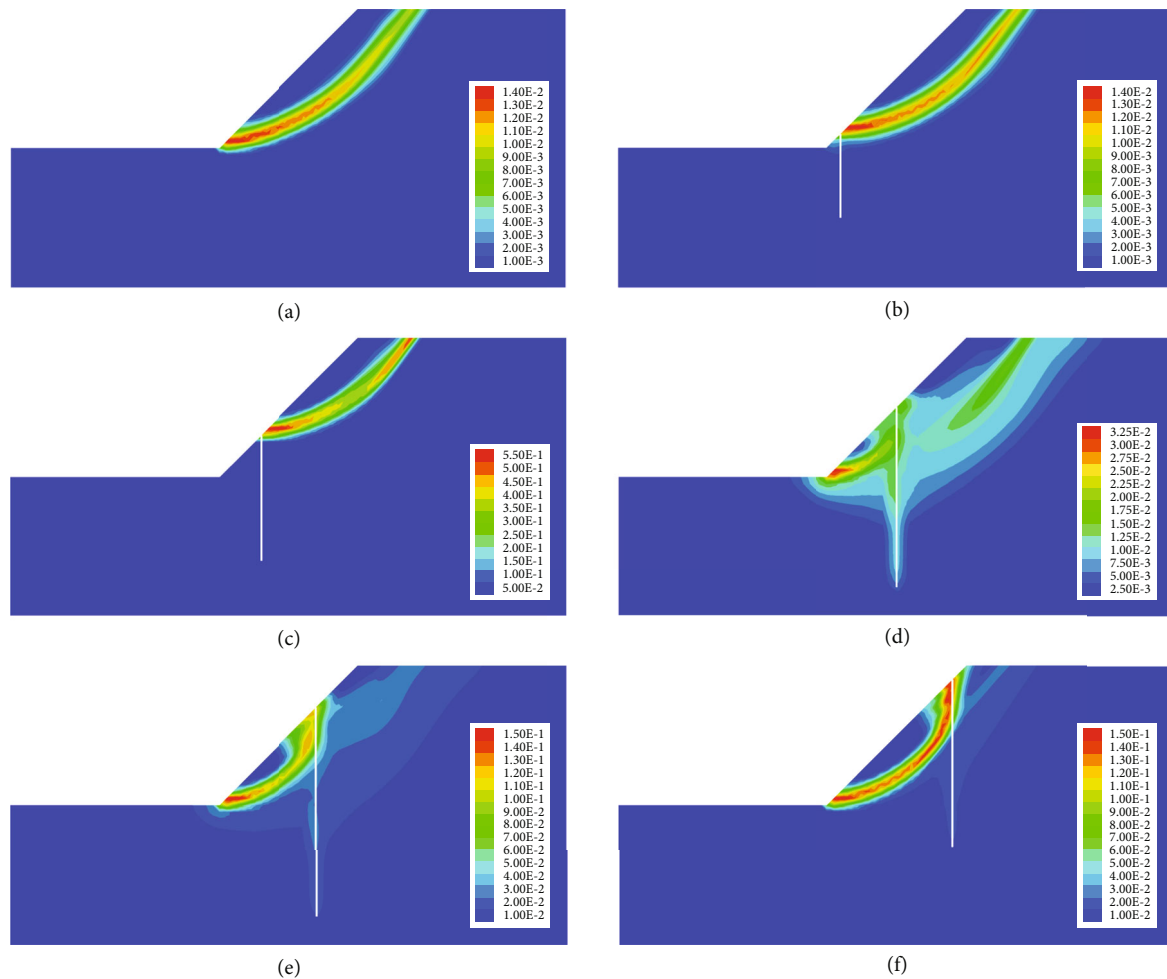
FIGURE 6: Maximum shear strain increment for various pile locations (the slope profile through the soil midway between the anti-slide piles). (a) without piles; (b) $L_x/L_p = 0.1$, pile length $L = 12$ m; (c) $L_x/L_p = 0.3$, pile length $L = 18$ m; (d) $L_x/L_p = 0.5$, pile length $L = 28$ m; (e) $L_x/L_p = 0.7$, pile length $L = 30$ m; (f) $L_x/L_p = 0.9$, pile length $L = 24$ m (taking the pile spacing of $S = 5$ m as an example). For interpretation of the references to color in this figure, the reader is referred to the electronic version of this page.

The value of $k_{(j)}$ determines the optimal membership degree of different schemes. Generally, the larger the value $k_{(j)}$ is, the more reasonable the scheme is.

## 3. Determination of Optimization Indexes and Values by Numerical Simulation

As mentioned above, the factor of safety, bending moment, shear force, and deflection of anti-slide piles are selected as the target value for the optimization design of anti-slide piles, which will be significantly affected by the reinforcement options such as pile lengths, pile location, and pile spacing [3]. The precise acquisition of optimization values is the key premise of comprehensive optimization. Therefore, the numerical simulation method is applied to obtain the accurate optimization index value and verify the reliability of the proposed model.

*3.1. Establishment of Numerical Model.* The homogeneous slope models considered by many researchers [3, 4, 11] were

adopted and established by the finite difference software FLAC[3D] except for some changes in the dimensions and gradients of slope as shown in Figure 2. Various reinforced schemes with anti-slide piles were designed considering different pile locations, pile lengths, and pile spacings. The uniform boundary conditions follow: The displacement of the bottom boundary is completely fixed, the horizontal displacement of the left and right boundary is restrained, and the upper boundary is free to move. Mohr-Coulomb constitutive model was selected to simulate the deformation and failure behavior of slope soil. The initial stress field only considers the self-weight stress field. The entire run-through of the plastic zone is regarded as the criterion of slope instability. Details about the parameters of soil are shown in Table 1. The factor of safety was calculated via the strength reduction method (SRM) [29–31].

Considering that the internal force of any section cannot be obtained directly with the solid element piles, and the accuracy of the calculating results is affected by the mesh size [32], the structural element pile was used to
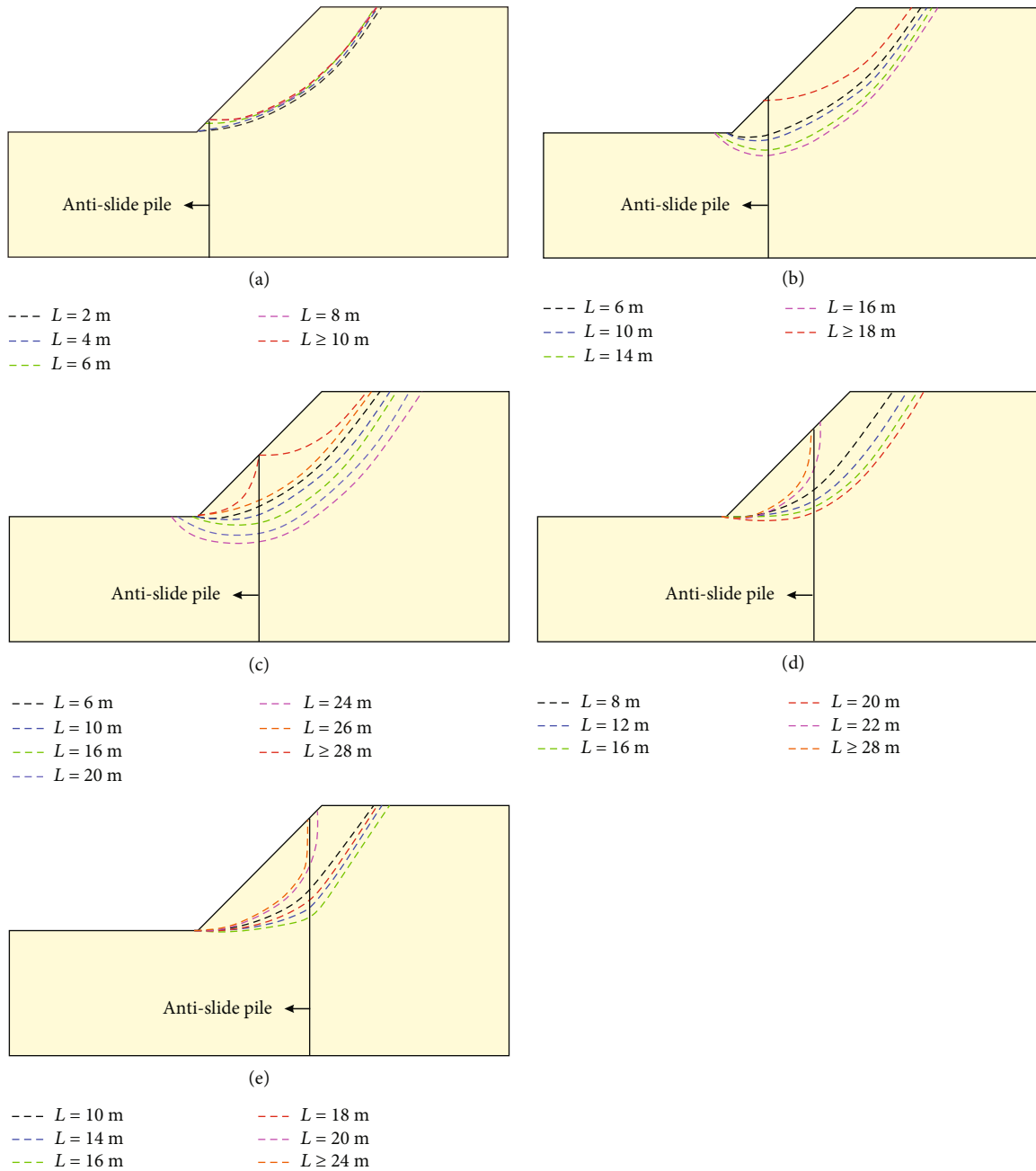
Figure 7: The critical slip surface for various pile lengths and pile locations. (a) $L_x/L_p = 0.1$; (b) $L_x/L_p = 0.3$; (c) $L_x/L_p = 0.5$; (d) $L_x/L_p = 0.7$; (e) $L_x/L_p = 0.9$ (taking the pile spacing of $S = 5$ m as an example). For interpretation of the references to color in this figure, the reader is referred to the electronic version of this page.

simulate the anti-slide pile with a cross-sectional dimension of $2$ m × $3$ m (width × height) due to the advantages of easy modeling, high calculation efficiency, and guaranteed accuracy [13, 33]. The mechanical model of the pile structural element is shown in Figure 3; the transfer of force and bending moment between the pile element and the mesh element could be realized by the normal coupling spring (Spring A) and the shear coupling spring (Spring B) at the position of the structural element node, which realizes the coupling effect between pile and soil. Details about the parameters of anti-slide piles are shown in Table 2.

3.2. Influence of Anti-Slide Pile Location on Slope Reinforcement. The influence of the anti-slide pile reinforcement location on the optimization indexes was studied with the pile spacing of 5 m. The pile location is defined by the ratio of the pile horizontal distance from the slope toe ($L_x$) to the horizontal length of the slope ($L_p$), which is shown in Figure 2. The effects of various pile locations and pile lengths on the factor of safety of the slope reinforced with piles are shown in Figure 4, and the maximum factor of safety for each pile location is shown in Figure 5. It can be obtained from Figures 4 and 5 that the factor of safety is the
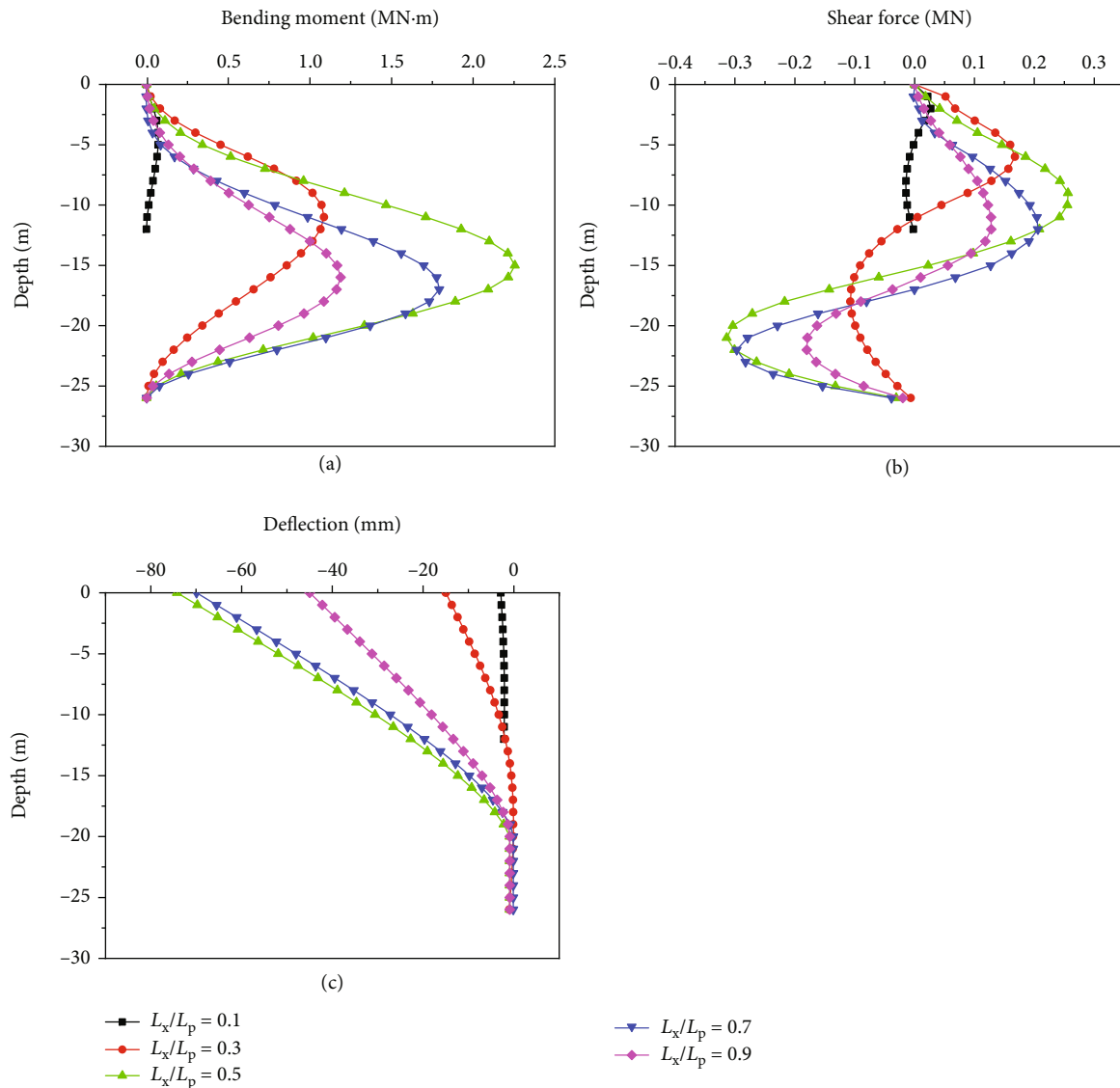
FIGURE 8: Anti-slide pile behaviors for various pile locations. (a) Bending moment. (b) Shear force; and (c) Deflection. For interpretation of the references to color in this figure, the reader is referred to the electronic version of this page.

largest and the reinforcement effect is the best when the anti-slide pile is located in the middle of the slope ($L_x/L_p = 0.5$); on the contrary, the factor of safety is the smallest, and the reinforcement effect is poor when the pile location is at the toe of the slope ($L_x/L_p = 0.1$). The results obtained in present research are similar to those of Cai and Ugai [3], Griffiths et al. [13], and Yang et al. [22].

The distribution of the shear strain increment zone is consistent with the large deformation area of the slope, which can reflect the position of the critical slip surface precisely. The effect of various pile locations on the maximum shear strain increment and the position of the critical slip surface obtained by FISH language is shown in Figures 6 and 7, respectively. It is seen from Figures 6 and 7 that the change of pile location has a significant impact on the distribution of critical slip surface. In other words, the concentration region of shear strain increment

and the run-through critical slip surface tends to form behind the anti-slide piles gradually when the pile location is located at the lower-middle part of the slope ($L_x/L_p = 0.1, 0.3$); however, the concentration region of shear strain increment and the run-through critical slip surface tends to form in front of the anti-slide piles eventually when the pile location is located at the upper-middle part of the slope ($L_x/L_p = 0.7, 0.9$). Therefore, it is concluded that there are three different failure modes of slope reinforced with piles. These failure modes are as follows: (1) slide will originate from the posterior surface of the piles when the pile location is located in the lower-middle part; (2) the critical slip surface is divided into two disconnected parts and slide is not easy to originate when the pile location is locked in the middle part; and (3) slide will originate from anterior of the piles when the pile location is located in the upper-middle part.
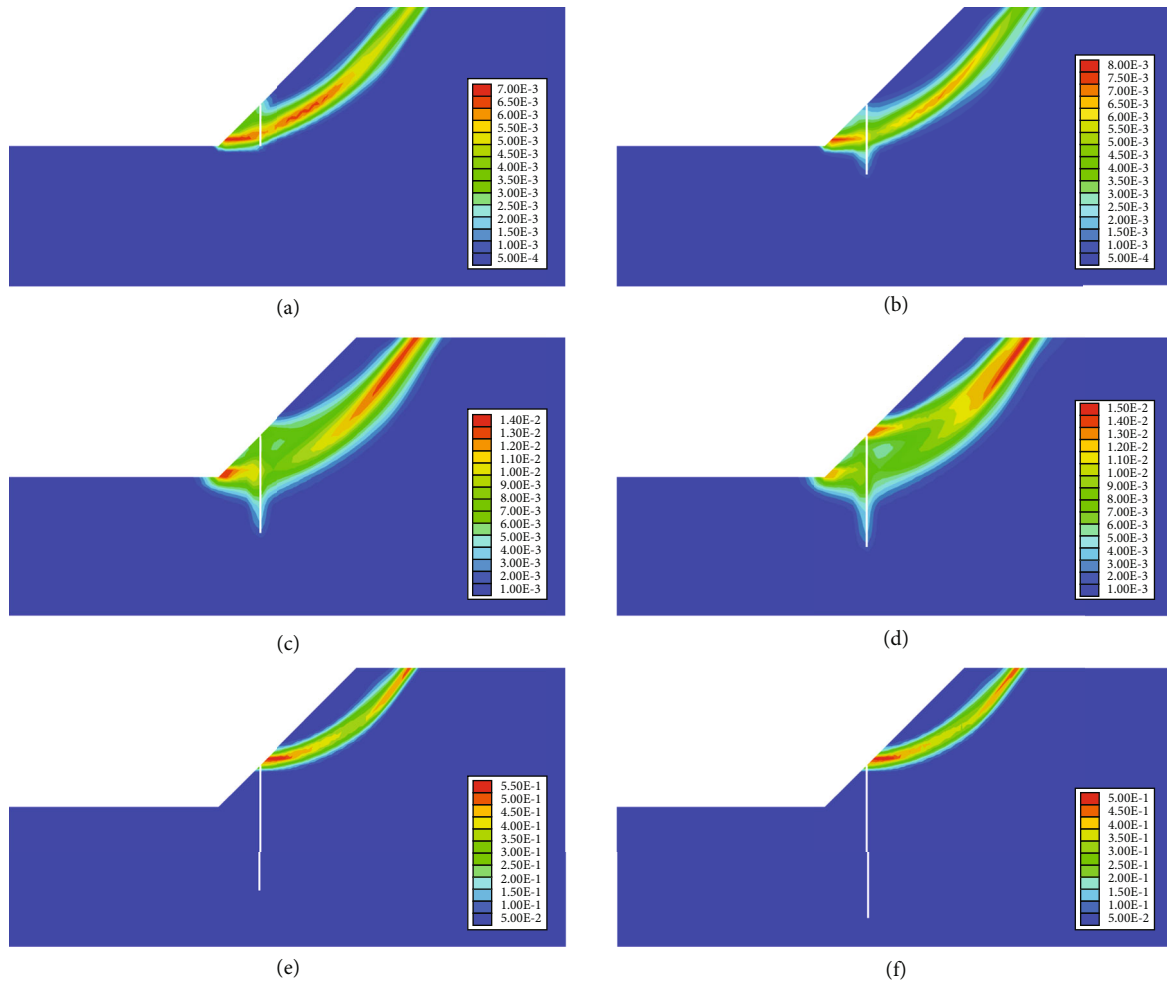
FIGURE 9: Maximum shear strain increment for various pile lengths (the slope profile through the soil midway between the anti-slide piles). (a) Pile length $L = 6$ m. (b) Pile length $L = 10$ m. (c) Pile length $L = 14$ m. (d) Pile length $L = 16$ m. (e) Pile length $L = 18$ m. (f) Pile length $L = 22$ m (taking the pile location of $L_x/L_p = 0.3$ and the pile spacing of $S = 5$ m as an example). For interpretation of the references to color in this figure, the reader is referred to the electronic version of this page.

The effect of various pile locations on behaviors of anti-slide piles is shown in Figure 8. The bending moment, the shear force, and the deflection of the pile increase at first and then decrease with the pile location from the toe upwards to the crest of the slope, and the maximum points of both pile behaviors appear in the pile located at the middle part of the slope. It should be noted that the depth of maximum bending moment or the shear force valued zero at each pile location has a good correspondence with the position of the critical slip surface. Thus, the various pile locations not only affect the factor of safety of the slope reinforced but also change the distribution of the interforce of piles.

### 3.3. Influence of Anti-Slide Pile Length on Slope Reinforcement.
The determination of pile length is the key to the optimization design of anti-slide piles. Too short pile length is not conducive to slope stability [19], and too long pile length will increase the engineering costs [22]. Figure 4 shows the effect of the pile length on the factor of safety of

the slope reinforced with anti-slide piles. Taking the pile location of $L_x/L_p = 0.3$ as an example, as expected, the factor of safety of the reinforced slope increases with increasing the pile length. However, when the pile length exceeds a certain length (18 m in the present study) which is named the critical pile length [13], the factor of safety is close to a constant gradually, and this is because enough anti-sliding force can be provided by the embedded length of piles in stable stratum to resist the sliding force.

In order to further study the effect of various pile lengths on the slope reinforcement, the maximum shear strain increment and the critical slip surface are obtained at the pile location of $L_x/L_p = 0.3$, as shown in Figures 7(b) and 9. It can be observed that with increasing the pile length, the zone of maximum shear strain increment is gradually divided into two parts that are not disconnected, but when the pile length exceeds 18 m, the run-through zone of maximum shear strain increment is reformed (Figures 9(e) and 9(f)). As shown in Figure 7(b), the critical slip surface becomes deeper with increasing the pile length, and the failure mode of
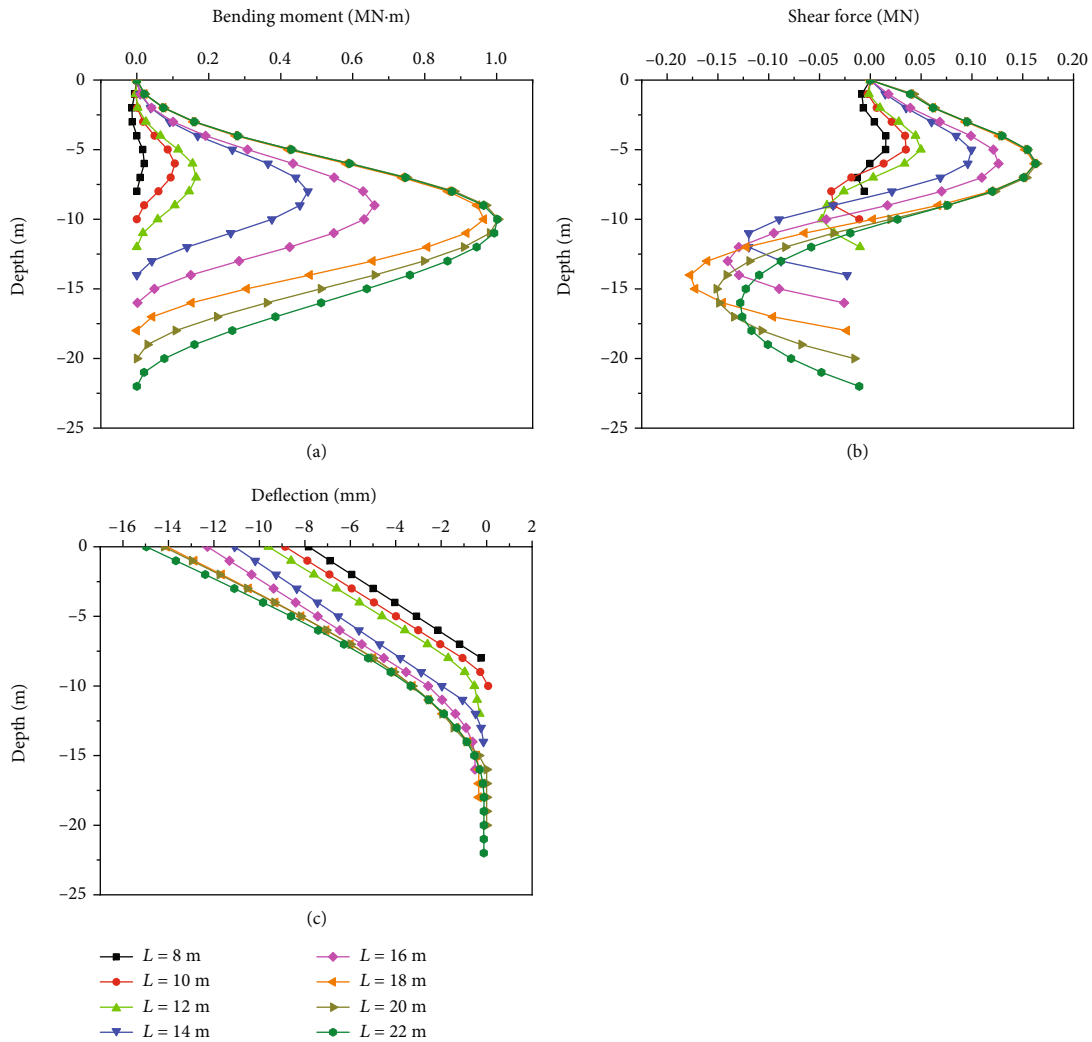
FIGURE 10: Anti-slide pile behaviors for various pile lengths. (a) Bending moment. (b) Shear force. (c) Deflection. For interpretation of the references to color in this figure, the reader is referred to the electronic version of this page.

reinforced slope changes from shallow sliding to deep sliding. This is mainly because the complex structure formed by pile-soil interaction improves the strength of soil around the pile. However, when the pile length is more than 18 m, the critical slip surface suddenly becomes shallow and passes through the top of the pile. The main reason for this is that deep sliding needs more energy due to the reinforcement of anti-slide piles, while shallow sliding only requires less energy to produce.

The effect of various pile lengths on the pile behaviors is shown in Figure 10. It can be seen that, when the pile length is less than the critical pile length (18 m), the bending moment (Figure 10(a)) increases with increasing the pile length and the position of the maximum bending moment is continuously away from the top of piles, which corresponds well to the position of the critical slip surface (Figure 7(b)); the positive shear force of piles (Figure 10(b)) increases as the pile length increases; the pile deflection increases with increasing of the pile length, but it should be noted that the distribution of deflection is almost linearly (Figure 10(c)) when the pile length is short, which indicates
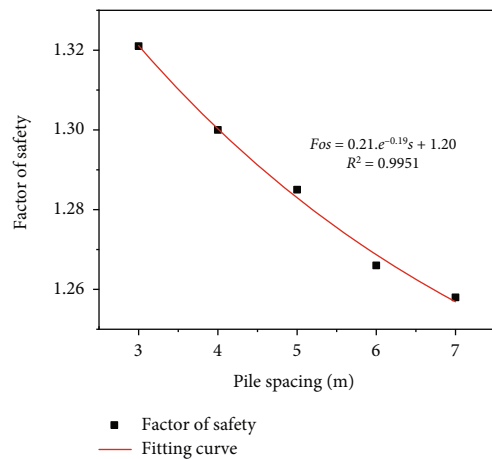


FIGURE 11: Factors of safety for various pile spacings under the critical pile length. *Fos* and *S* stand for the factor of safety and the pile spacing, respective. For interpretation of the references to color in this figure, the reader is referred to the electronic version of this page.
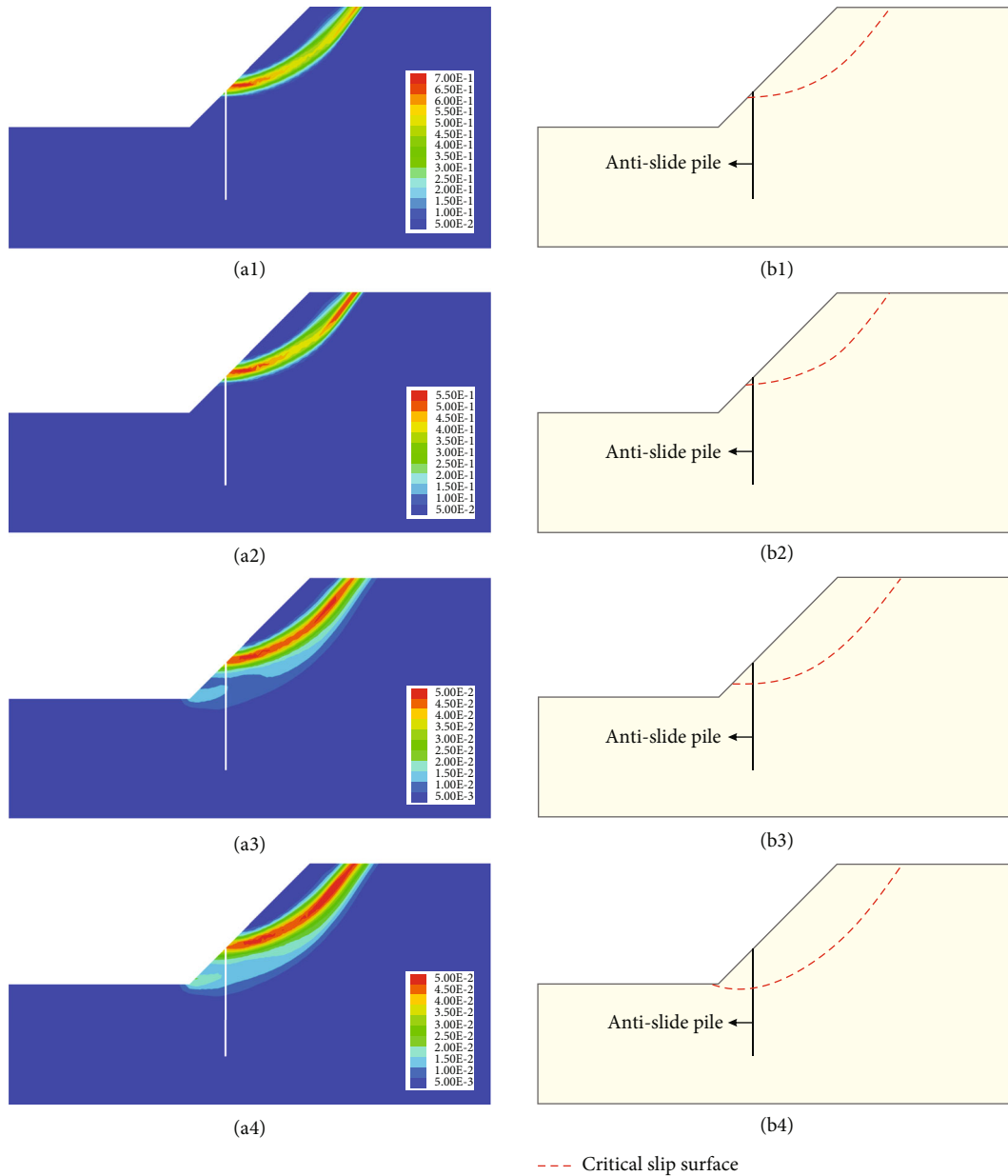
FIGURE 12: Contour of shear strain increment and the critical slip surface for various pile spacings under the critical pile length (the slope profile through the soil midway between the anti-slide piles). (a1), (b1) Pile spacing S = 4 m. (a2), (b2) Pile spacing S = 5 m; (a3), (b3) Pile spacing S = 6 m; (a4), (b4) Pile spacing S = 7 m (taking the pile location of $L_x/L = 0.3$ and the critical pile length ($L = 18$ m) as an example). For interpretation of the references to color in this figure, the reader is referred to the electronic version of this page.

that the pile is prone to overturning failure under too short pile length. When the pile length exceeds the critical pile length, the bending moment, shear force, and deflection all tend to be a stable distribution, which is consistent with the change law of the factor of safety.

### 3.4. Influence of Anti-Slide Pile Spacing on Slope Reinforcement.
Taking the pile location of $L_x/L_p = 0.3$ and the critical pile length (18 m) as an example, the effect of various pile spacings on the reinforced slope is studied. Figure 11 shows the change of factors of safety under various pile spacings; it can be seen that the factor of safety

of the reinforced slope decreases with increasing the pile spacing.

The effects of various pile spacings on the maximum shear strain increment and the critical slip surface are shown in Figure 12. It can be seen that when the pile spacing is small, the critical slip surface between two anti-slide piles is shallow and almost passes over the top of the pile. With increasing the pile spacing, the critical slip surface gradually becomes deeper, and the instability mode has changed. When the pile spacing is large enough (Figure 12(a4)), a complete and run-through critical slip surface is formed gradually, which is nearly close to the critical slip surface of the slope unreinforced (Figure 6(a)). This may be
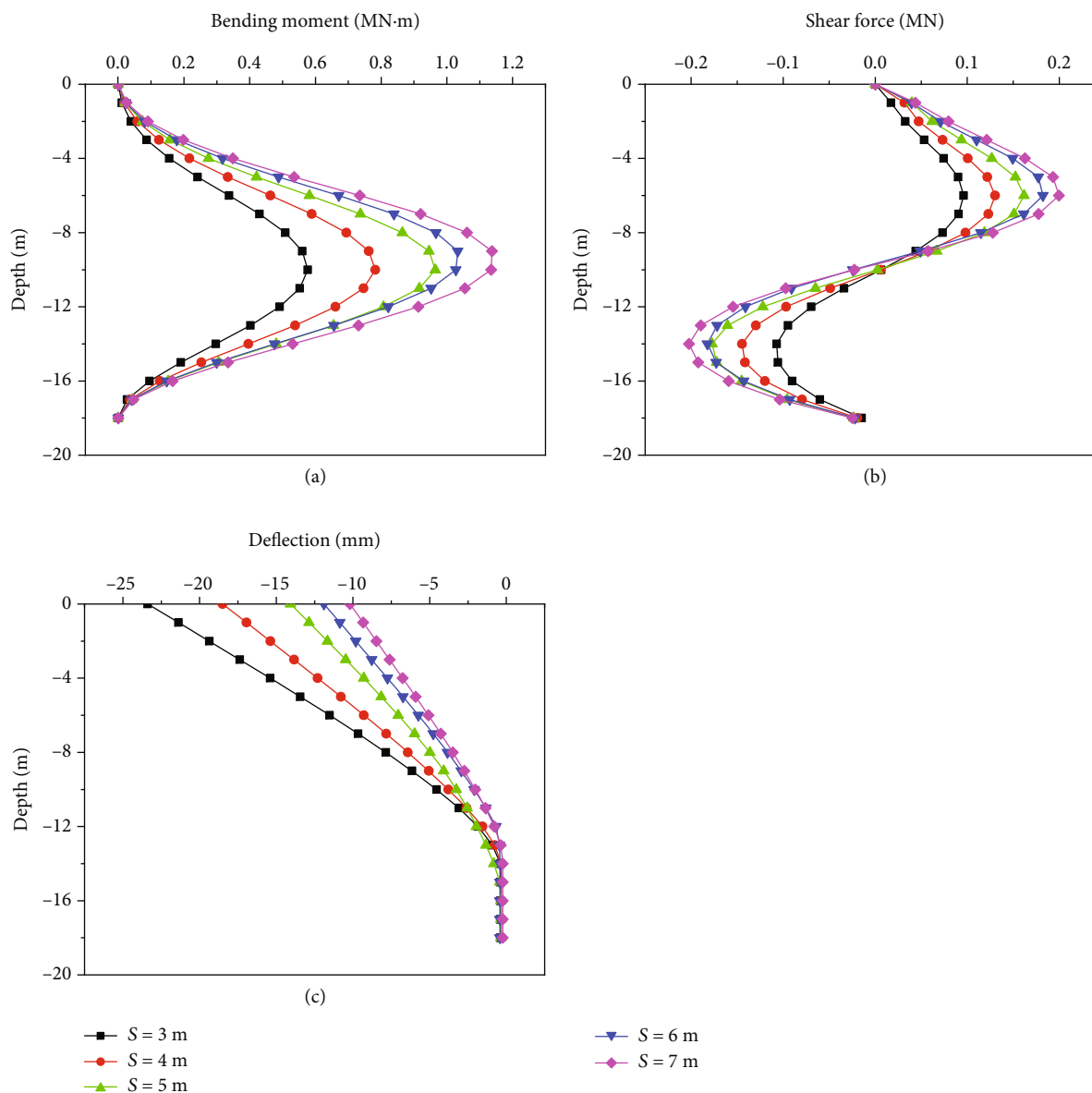
FIGURE 13: Pile behaviors for various pile spacings under the critical pile length. (a) Bending moment. (b) Shear force. (c) Deflection. For interpretation of the references to color in this figure, the reader is referred to the electronic version of this page.

related to the evolution of soil arch under various pile spacings.

The effect of various pile spacings on the pile behaviors is shown in Figure 13. It can be concluded that the bending moment (Figure 13(a)) and the shear force (Figure 13(b)) increase with increasing the pile spacing. This can be explained by the fact that the anti-slide piles act as the retaining walls and the integrity and strength of the pile and soil are improved significantly while the pile spacing decreases so that soil would not reach the limit state until the soil with large deformation [3], which can be demonstrated by the pile deflection (Figure 13(c)); soil arch between piles disappears gradually when the pile spacing increases, and only a single anti-slide pile works at this moment.

To sum up, the interaction between pile and soil is fully considered with the numerical simulation method,

and the factor of safety, bending moment, shear force, and deflection of anti-slide piles obtained under various reinforcement options are more realistic, which is in good agreement with previous studies [3, 18, 34]. Therefore, it is feasible to obtain the optimization index values by the numerical simulation and to optimize designs combined with the proposed multi-objective comprehensive optimization model.

## 4. Results and Discussion

The factor of safety and the bending moment, shear force, and deflection of piles were obtained based on the numerical simulation under various reinforcement schemes, and results were analyzed with the proposed multi-objective comprehensive optimization model.

| Optimization indexes | Factor of safety | Bending moment | Shear force | Deflection | Subjective weight |
|---|---|---|---|---|---|
| Factor of safety | 1 | 3 | 7 | 6 | 0.5570 |
| Bending moment | 1/3 | 1 | 5 | 4 | 0.2693 |
| Shear force | 1/7 | 1/5 | 1 | 1/4 | 0.0532 |
| Deflection | 1/6 | 1/4 | 4 | 1 | 0.1205 |

### 4.1. Results Analysis

*4.1.1. Calculation Results of Indicator Value and Weight.* The indicator value of the optimization system was determined by the numerical simulation. It should be noted that the factor of safety of reinforced slope belongs to the positive optimization index, and the bending moment, shear force and deflection belong to the negative optimization indexes, so Equations (1) and (2) are used for normalization calculation, respectively. The calculation results of indicator values under different reinforcement schemes are shown in Tables S1-S5 in Supplemental Files.

Decision-making AHP method was adopted to determine the subjective weight of optimization indexes. Considering intentions of decision-makers, engineering experience, and judgements of geological hazard experts, 1-9 ratio scaling method was taken to define the relative importance and subjective weight of each optimization index, as shown in Table 3. According to the principle of AHP [35], the maximum eigenvalue of judgment matrix ($\lambda_{\max}$) is 4.25, the consistency index (CI) is 0.08, and the consistency ratio (CR) equals 0.09 and is less than 0.1, which meets the consistency requirements.

The objective weight is calculated by Equation (5) based on the entropy method, and the results are shown in Table 4.

The comprehensive weight of each evaluating index is calculated via Equation (4) as shown in Table 4. Among them, the weight of the factor of safety is the largest, and the shear force of pile is the smallest.

*4.1.2. Optimal Results Analysis.* The fuzzy comprehensive optimization value $k_{(j)}$ is calculated according to Equation (6) (where $\alpha = 60$ and $\beta = 40$). The comprehensive optimization results are shown in Figure 14. It can be seen that the results under various reinforcement schemes are significantly different. According to the principle of optimal judgment, the comprehensive optimization value corresponding to scheme 35 is the highest, that is, the anti-slide pile located in the middle of slope, with a pile length of 28 m and pile location of 4 m, is the most reasonable choice. In addition, more details could be drawn as follows.

(1) When anti-slide piles are located in the middle or upper-middle part ($L_x/L_p = 0.7$) of the slope, the effect of the slope reinforced with piles is obviously better than that of the toe or crest of the slope, which is in good agreement with the numerical simulation (Section 3.2) and results obtained by Hassiotis et al. [1] and Yang et al. [36]

TABLE 4: Comprehensive weight determination for optimization indexes.

| Optimization indexes | Subjective weight | Objective weight | Comprehensive weight |
|---|---|---|---|
| Factor of safety | 0.5570 | 0.3984 | 0.7216 |
| Bending moment | 0.2693 | 0.1485 | 0.1301 |
| Shear force | 0.0532 | 0.1334 | 0.0231 |
| Deflection | 0.1205 | 0.3197 | 0.1252 |

(2) The increase in pile length can significantly improve the reinforcement effect of the slope, but it does not mean that the longer the pile length, the better the reinforcement effect. For example, when the pile is located in the lower-middle part ($L_x/L_p = 0.3$) with the pile spacing of 5 m, the value of $k_{(j)}$ increases slightly or even decreases when the pile length exceeds 18 m (Figure 14); this is mainly because excessive pile length leads to the increase of internal force of anti-slide piles under the premise of meeting design requirements of the factor of safety, which is not conducive to the safety of piles

(3) The smaller pile spacing is, the better reinforcement effect is. In addition, the reinforcement effect of piles located in the location of $L_x/L_p = 0.7$ with pile spacing of 5 m is significantly better than that in the location of $L_x/L_p = 0.5$ with pile spacing of 6 m; therefore, the pile spacing can be appropriately reduced to improve the reinforcement effect in actual engineering when the anti-pile is located in non-middle position

### 4.2. Discussion

*4.2.1. Comparisons with Results under Various $\alpha$ and $\beta$ Values.* In order to make the evaluating indexes more comparable and keep as much information as possible about the changes in the optimization index values, the constants $\alpha$ and $\beta$ were introduced to construct the normalization functions (Equations (1) and (2)) based on the percentage system. Figure 15 presents the effect of various combinations of $\alpha$ and $\beta$ on the optimization results of anti-slide piles. The result indicates that curves of the optimization result under various values of $\alpha$ and $\beta$ present the approximately parallel relationship and have exactly the same changing law. Besides, the larger the value of $\alpha$ is, the greater the
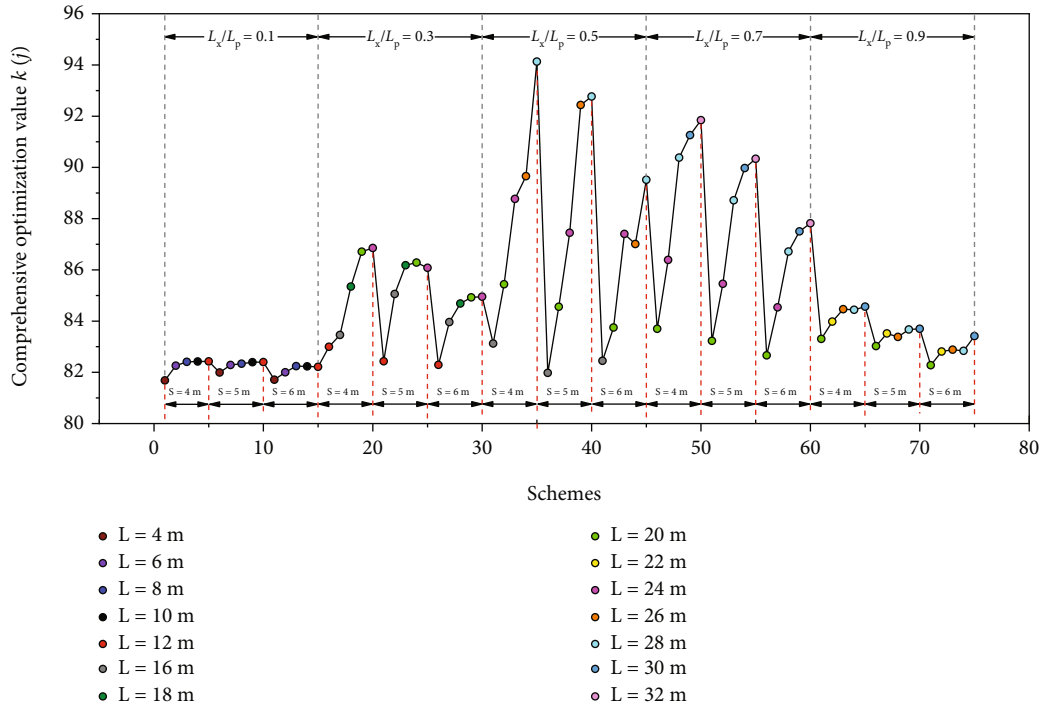
FIGURE 14: Optimization results based on the multi-objective comprehensive optimization model. $S$ and $L_x/L_p$ stand for the pile spacing and the pile location, respectively. For interpretation of the references to color in this figure, the reader is referred to the electronic version of this page.
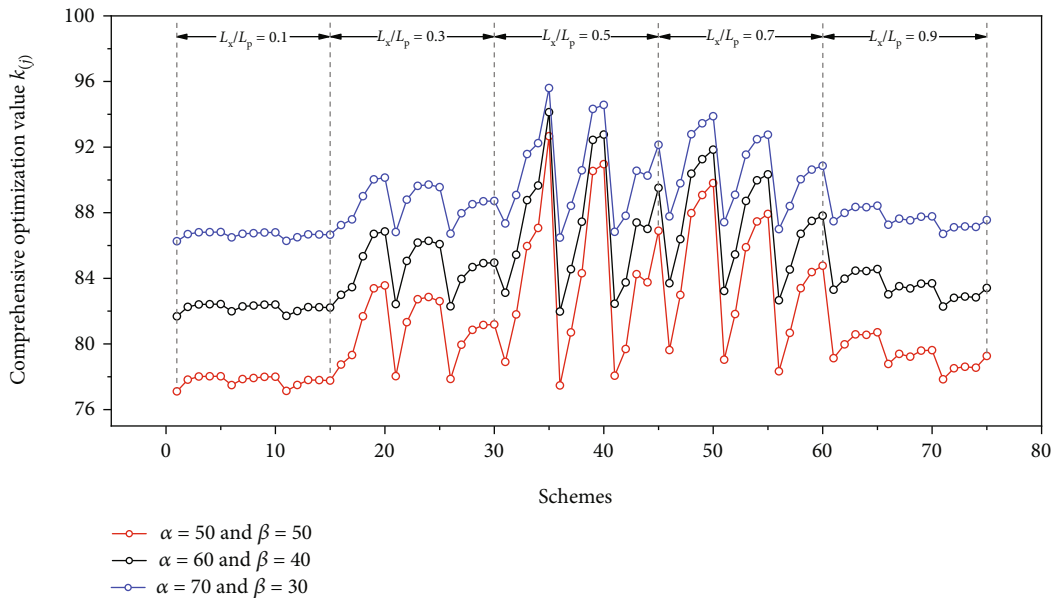


FIGURE 15: Comparison of optimization results with different $\alpha$ and $\beta$ values (refer to Tables S1-S5 in Supplemental Files or Figure 14 for detailed reinforcement scheme corresponding to scheme number). For interpretation of the references to color in this figure, the reader is referred to the electronic version of this page.

optimization value for the corresponding scheme. However, the changes of $\alpha$ and $\beta$ only change the absolute value of optimization results and amplitude of variation of curves but have no effects on the final optimization results.

4.2.2. Comparisons with Results under Various Weights. The final optimization results under comprehensive weight, subjective weight, and objective weight are shown in Figure 16. It can be seen that the result (red line in Figure 16) by using
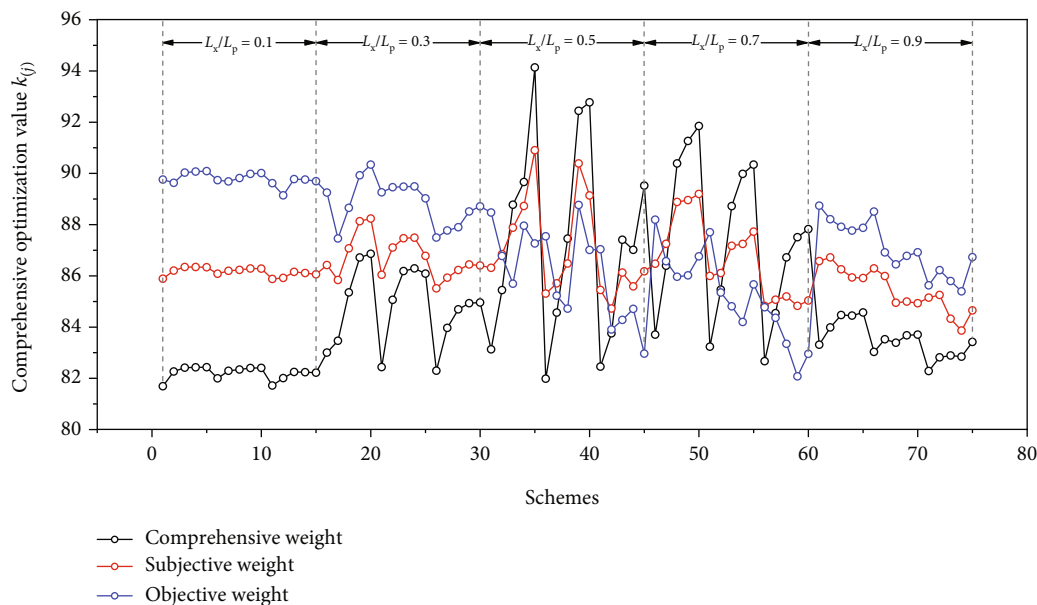
FIGURE 16: Comparison of optimization results with different weights (refer to Tables S1-S5 in Supplemental Files or Figure 14 for detailed reinforcement scheme corresponding to scheme number). For interpretation of the references to color in this figure, the reader is referred to the electronic version of this page.

the subjective weight only indicates that scheme 35 is the optimal reinforcement option, which is basically consistent with the conclusion drawn via the proposed method in this article, but the optimization values of each scheme have little difference, which is easy to make wrong decisions due to the human factors implications and inaccurate data. The optimization result (blue line in Figure 16) obtained only by the objective weight reveals that the reinforcement effect is the worst when the anti-slide pile is located in the middle part of the slope, which is totally at variance with the practical engineering experience; this may be the reason that the index weight of entropy method is determined according to the variation degree of the index, which ignores the importance of the index itself. A comparison of the three different optimization results shows that the comprehensive weight proposed in this article makes the optimization results more scientific and reasonable. Therefore, with the continuous development of habitable earth construction, the proposed multi-objective comprehensive optimization model will play an important role in the design of slope reinforcement.

*4.2.3. Limitation of the Proposed Method.* In the current study, the numerical simulation method was used to obtain the values of evaluating indexes in the multi-objective comprehensive optimization model. Although more reasonable optimization results had been achieved, more engineering cases and field monitoring data are still needed to further study to verify the accuracy and applicability of this proposed model. Besides, the comprehensive weight used in this article considers the advantages of both subjective and objective weight and minimizes the adverse effects of shortcomings of two on optimization results, but it is still unavoidable that the weight obtained goes against the actual

situation, which leads to make an absurd decision-making. Therefore, it is necessary to further optimize the index weight based on methods of big data, machine learning, and deep learning. Besides, we note that multilayered structures of slopes significantly change the distribution of critical slip surfaces and the actual force situation of anti-slide piles. Further, these changes are more visually reflected in the variation of the factor of safety, deflection, bending moment, shear force, and so on. These parameters are consistent with the evaluation index system in new optimization model. Therefore, the proposed new evaluation optimization model could be applied to the optimal design of anti-slide piles in multilayer complex slopes in theory. A further research could be focused on the applicability of the new optimization method in more complex types of slopes.

*4.2.4. Research Prospect.* The deterministic analysis method was used in a multi-objective comprehensive optimization model to solve the optimization design parameters based on the numerical simulation. In fact, the physical and mechanical parameters of slopes or anti-slide piles exhibit strong heterogeneity affected by temperature, gravity stress, and spatial distribution [37]. For example, the cohesion usually shows an increasing trend while for internal friction angle a decreasing trend with soil depth due to the increase of confining pressure [38]. Previous research related to the optimal design of anti-slip pile reinforced slopes has shown that the results of slope stability, the evolution of slip surface, and the failure modes considering the friction and cohesion of slope soil as lognormally distributed random variables and the compression strength and pile width as normally distributed random variables are more consistent with the reality compared with the deterministic model [39]. Therefore, a further modification could be focused on the

influence of the selection of random variables (e.g., sensitivity analysis), the distribution type of random variables (e.g., Gaussian distribution or Weibull distribution), the variation coefficient, the multilayer structure of slope on the slope stability, and the optimization design of anti-slide pile, which to obtain more accurate and repeatable optimization index parameters, make objective and comprehensive optimization evaluation, and provide the more reasonable reinforcement schemes. In addition, how to combine the advanced geotechnical probabilistic methods, such as the Monte Carlo simulation (MCS) [40], the first-order reliability method (FORM) [41], and weighted uniform simulation [42, 43], with our comprehensive optimization model to improve the efficiency of optimization should be properly dealt with in future studies.

## 5. Conclusion

The multi-objective comprehensive optimization model for the design of slope reinforced with anti-slide piles was proposed based on the fuzzy comprehensive evaluation method, and the reliability of the model was verified by finite difference numerical simulation. The main conclusions are as follows:

(1) According to the numerical simulation results, various pile locations, pile lengths, and pile spacings have significant effects on the slope reinforced. The best reinforcement effect could be obtained when the pile is located in the middle part of the slope. The increase of the pile length can increase the reinforcement effect obviously, but it will not continue to increase the slope stability when the pile length exceeds the critical pile length. The larger the pile spacing is, the worse the stability of the slope and safety of the anti-slide pile is

(2) The factor of safety, bending moment, shear force, and deflection of the anti-slide pile were selected as the optimization index system to ensure that the optimized reinforcement scheme could meet the stability of the pile-slope system. Meanwhile, the comprehensive weight was determined combined with the subjective and objective, which is more in line with practical engineering cases

(3) Based on the three-dimensional slope numerical model, the proposed multi-objective comprehensive optimization model was applied to optimize various reinforcement schemes, which obtained reasonable optimization results. This provides a new solution for the optimization design of other types of complex slopes and has broad application prospects

## Data Availability

The data used to support the findings of this study are available from the corresponding author upon request.

## Disclosure

A preprint version of the research is available at Research Square [44].

## Conflicts of Interest

The authors declare that they have no known competing financial interests or personal relationships that could have appeared to influence the work reported in this paper.

## Acknowledgments

## Supplementary Materials

Table S1. The standardized values of optimization indexes (pile location $L_x/L_p = 0.1$). Table S2. The standardized values of optimization indexes (pile location $L_x/L_p = 0.3$). Table S3. The standardized values of optimization indexes (pile location $L_x/L_p = 0.5$). Table S4. The standardized values of optimization indexes (pile location $L_x/L_p = 0.7$). Table S5. The standardized values of optimization indexes (pile location $L_x/L_p = 0.9$). *(Supplementary Materials)*

## References

[1] S. Hassiotis, J. L. Chameau, and M. Gunaratne, "Design method for stabilization of slopes with piles," *Journal of Geotechnical and Geoenvironmental Engineering*, vol. 123, no. 4, pp. 314–323, 1997.

[2] C. D. Li, W. Q. Chen, Y. J. Song, W. P. Gong, and Q. H. Zhao, "Optimal location of piles in stabilizing slopes based on a simplified double-row piles model," *KSCE Journal of Civil Engineering*, vol. 24, no. 2, pp. 377–389, 2020.

[3] F. Cai and K. Ugai, "Numerical analysis of the stability of a slope reinforced with piles," *Soils and Foundations*, vol. 40, no. 1, pp. 73–84, 2000.

[4] W. B. Wei and Y. M. Cheng, "Strength reduction analysis for slope reinforced with one row of piles," *Computers and Geotechnics*, vol. 36, no. 7, pp. 1176–1185, 2009.

[5] S. Kanagasabai, J. Smethurst, and W. Powrie, "Three-dimensional numerical modelling of discrete piles used to stabilize landslides," *Canadian Geotechnical Journal*, vol. 48, no. 9, pp. 1393–1411, 2011.

[6] V. E. Price and N. R. Morgenstern, "The analysis of The stability of general slip Surfaces," *Geotechnique*, vol. 18, no. 3, pp. 393-394, 1968.

[7] C. Viggiani, "Ultimate lateral load on piles used to stabilize landslides," *International Journal of Rock Mechanics and Mining Sciences & Geomechanics Abstracts*, vol. 21, no. 3, pp. 555–560, 1981.

[8] T. Ito and T. Matsui, "Methods to estimate lateral force acting on stabilizing piles," *Soils and Foundations*, vol. 15, no. 4, pp. 43–59, 1975.

[9] H. Poulos, "Analysis of piles in soil undergoing lateral movement," *Journal of the Soil Mechanics and Foundations Division*, vol. 99, no. 5, pp. 391–406, 1973.

[10] T. K. Nian, G. Q. Chen, M. T. Luan, Q. Yang, and D. F. Zheng, "Limit analysis of the stability of slopes reinforced with piles against landslide in nonhomogeneous and anisotropic soils," *Canadian Geotechnical Journal*, vol. 45, no. 8, pp. 1092–1103, 2008.

[11] J. Won, K. You, S. Jeong, and S. Kim, "Coupled effects in stability analysis of pile–slope systems," *Computers and Geotechnics*, vol. 32, no. 4, pp. 304–315, 2005.

[12] E. Ausilio, E. Conte, and G. Dente, "Stability analysis of slopes reinforced with piles," *Computers and Geotechnics*, vol. 28, no. 8, pp. 591–611, 2001.

[13] D. V. Griffiths, H. Lin, and P. Cao, "A comparison of numerical algorithms in the analysis of pile reinforced slopes," in *Geo-Florida 2010: Advances in Analysis, Modeling and Design Conference*, pp. 175–183, West Palm Beach, Florida, USA, 2010.

[14] I. Shooshpasha and H. A. Amirdehi, "Evaluating the stability of slope reinforced with one row of free head piles," *Arabian Journal of Geosciences*, vol. 8, no. 4, pp. 2131–2141, 2015.

[15] F. Y. Chen, R. H. Zhang, Y. Wang, H. Liu, T. Böhlke, and W. G. Zhang, "Probabilistic stability analyses of slope reinforced with piles in spatially variable soils," *International Journal of Approximate Reasoning*, vol. 122, pp. 66–79, 2020.

[16] M. Hajiazizi, M. Bavali, and A. Fakhimi, "Numerical and experimental study of the optimal location of concrete piles in a saturated sandy slope," *International Journal of Civil Engineering*, vol. 16, no. 10, pp. 1293–1301, 2017.

[17] J. Zhang, H. Wang, H. W. Huang, and L. H. Chen, "System reliability analysis of soil slopes stabilized with piles," *Engineering Geology*, vol. 229, pp. 45–52, 2017.

[18] S. Jeong, B. Kim, J. Won, and J. Lee, "Uncoupled analysis of stabilizing piles in weathered slopes," *Computers and Geotechnics*, vol. 30, no. 8, pp. 671–682, 2003.

[19] R. Kourkoulis, F. Gelagoti, I. Anastasopoulos, and G. Gazetas, "Slope stabilizing piles and pile-groups: parametric study and design insights," *Journal of Geotechnical and Geoenvironmental Engineering*, vol. 137, no. 7, pp. 663–677, 2011.

[20] C. D. Li, H. M. Tang, X. L. Hu, and L. Q. Wang, "Numerical modelling study of the load sharing law of anti-sliding piles based on the soil arching effect for Erliban landslide, China," *KSCE Journal of Civil Engineering*, vol. 17, no. 6, pp. 1251–1262, 2013.

[21] R. J. Li, W. Zheng, S. J. Shao, and K. Liu, "Analysis of local sliding mechanism of Longdong slope reinforced with stabilizing piles," *Rock and Soil Mechanics*, vol. 31, no. S2, pp. 322–327, 2010.

[22] S. K. Yang, X. H. Ren, and J. X. Zhang, "Study on embedded length of piles for slope reinforced with one row of piles," *Journal of Rock Mechanics and Geotechnical Engineering*, vol. 3, no. 2, pp. 167–178, 2011.

[23] C. C. Wang, J. T. Li, J. Liao, R. Q. Hao, and B. Liu, "Stability analysis of slope reinforced with piles and optimization," *Journal of Central South University (Science and Technology)*, vol. 46, no. 1, pp. 231–237, 2015.

[24] Y. Zhu, H. H. Zhu, W. Zhang, and B. Shi, "Parametric analysis on factors influencing stability of slopes reinforced by anti-slide piles," *Journal of Engineering Geology*, vol. 25, no. 3, pp. 833–840, 2017.

[25] J. C. Xu, "Analytic hierarchy process for assessing factors influencing the stability of soil slopes reinforced with piles," *Environmental Earth Sciences*, vol. 70, no. 4, pp. 1507–1514, 2013.

[26] Q. L. Li and H. W. Wei, "Optimization design of pile location on slope based on multi-objective comprehensive evaluation method," *Journal of Railway Science and Engineering*, vol. 15, no. 6, pp. 1445–1452, 2018.

[27] W. B. Zhao, Y. Q. Luo, and Y. Feng, "Study on designing system of anti-slide piles based on reliability theory," *Rock and Soil Mechanics*, vol. 27, no. S2, pp. 952–957, 2006.

[28] B. Liu, F. L. Zhang, W. Y. Wan, and X. W. Luo, "Multi-objective decision-making for the ecological operation of built reservoirs based on the improved comprehensive fuzzy evaluation method," *Water Resources Management*, vol. 33, no. 11, pp. 3949–3964, 2019.

[29] T. Matsui and K. C. San, "Finite element slope stability analysis by shear strength reduction technique," *Soils and Foundations*, vol. 32, no. 1, pp. 59–70, 1992.

[30] O. C. Zienkiewicz, C. Humpheson, and R. W. Lewis, "Associated and non-associated visco-plasticity and plasticity in soil mechanics," *Géotechnique*, vol. 25, no. 4, pp. 671–689, 1975.

[31] D. V. Griffiths and P. A. Lane, "Slope stability analysis by finite elements," *Géotechnique*, vol. 49, no. 3, pp. 387–403, 1999.

[32] C. Chen, W. Wang, and H. Y. Lv, "Stability analysis of slope reinforced with composite anti-slide pile model," *Rock and Soil Mechanics*, vol. 40, no. 8, pp. 3207–3217, 2019.

[33] F. H. Lee, S. H. Goh, and S. Banerjee, "Earthquake-induced bending moment in fixed-head piles in soft clay," *Geotechnique*, vol. 64, no. 6, pp. 431–446, 2014.

[34] M. Hajiazizi, A. Mazaheri, and R. Orense, "Analytical approach to evaluate stability of pile-stabilized slope," *Scientia Iranica*, vol. 25, no. 5, pp. 2525–2536, 2018.

[35] M. Brunelli, "Introduction and Fundamentals," in *Introduction to the Analytic Hierarchy Process*, Springer, Cham, 2015.

[36] G. H. Yang, Y. X. Zhang, Y. C. Zhang, and J. Z. Tang, "Optimal site of anti-landslide piles based on deformation field of slopes," *Chinese Journal of Geotechnical Engineering*, vol. 33, no. S1, pp. 8–13, 2011.

[37] A. Johari and A. Talebi, "Stochastic analysis of rainfall-induced slope instability and steady-state seepage flow using random finite-element method," *International Journal of Geomechanics*, vol. 19, no. 8, article 04019085, 2019.

[38] J. Ji, C. W. Wang, Y. F. Gao, and L. M. Zhang, "Probabilistic investigation of the seismic displacement of earth slopes under stochastic ground motion: a rotational sliding block analysis," *Canadian Geotechnical Journal*, vol. 58, no. 7, pp. 952–968, 2021.

[39] Q. Lü, B. Xu, Y. Yu et al., "A practical reliability assessment approach and its application for pile-stabilized slopes using FORM and support vector machine," *Bulletin of Engineering Geology and the Environment*, vol. 80, no. 8, pp. 6513–6525, 2021.

[40] H. J. Pradlwarter and G. I. Schuëller, "Local domain Monte Carlo simulation," *Structural Safety*, vol. 32, no. 5, pp. 275–280, 2010.

[41] J. Ji, C. S. Zhang, Y. F. Gao, and J. Kodikara, "Reliability-based design for geotechnical engineering: an inverse FORM

approach for practice," *Computers and Geotechnics*, vol. 111, pp. 22–29, 2019.

[42] J. Ji and L. P. Wang, "Efficient geotechnical reliability analysis using weighted uniform simulation method involving correlated nonnormal random variables," *Journal of Engineering Mechanics*, vol. 148, no. 6, article 06022001, 2022.

[43] M. Rashki, M. Miri, and M. Azhdary Moghaddam, "A new efficient simulation method to approximate the probability of failure and most probable point," *Structural Safety*, vol. 39, pp. 22–29, 2012.

[44] C. Xu, L. Xue, C. Cui et al., *A New Multi-Objective Comprehensive Optimization Model for Design of Anti-Slide Piles*, 2021.